

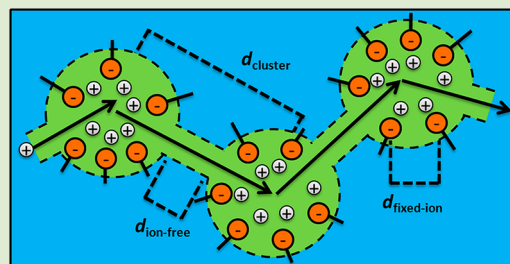
Design of Cluster-free Polymer Electrolyte Membranes and Implications on Proton Conductivity

Keith M. Beers^{†,‡} and Nitash P. Balsara^{*,†,‡,§}

[†]Materials Sciences Division and [§]Environmental Energy Technologies Division, Lawrence Berkeley National Laboratory, Berkeley, California 94720, United States

[‡]Department of Chemical Engineering, University of California, Berkeley, California 94720, United States

ABSTRACT: Nanoscale ionic aggregates are ubiquitous in copolymers containing charged and uncharged monomers. In most cases, these clusters persist when these polymers are hydrated and ion-conducting channels percolate through the sample. We argue that these clusters impede ion motion due to (1) the requirement that ions must hop across ion-free regions in the channels as they are transported from one cluster to the next, and (2) increased counterion condensation due to proximity of fixed acid groups in the clusters. Block copolymers wherein the size of the ion-containing microphase is 6 nm or less provides one approach for eliminating the clusters.



Significant research has been conducted on ion containing polymers because of their potential use as polymer electrolyte membranes (PEMs) in fuel cells,^{1,2} batteries,³ actuators,⁴ and solar energy conversion devices.^{5,6} Of particular interest are chains where a fraction of monomers are charged. One charge is bound to the backbone of the polymer chain while the other counterion is mobile. These materials are called single-ion conductors because only one of the ions carries current. An important consequence of this is the absence of concentration gradients during charge transport. This lowers the overpotential needed for operation of fuel cells, batteries, etc. The electrolyte in a fuel cell is an open system, wherein water contained in humid air fed at the cathode enters the membrane. Single-ion conductors are thus essential for fuel cell electrolyte applications because any added salt will eventually be washed out.

Ion containing polymers are also of commercial interest due to their unique mechanical properties. Dipole–dipole interactions between the ion pairs along the polymer chain, causes reversible clustering of ion-rich moieties within a nonpolar polymer matrix. These ionomers, which typically contain a heavy metal cation, are robust solids due to the fact that the clusters act as physical cross-links between polymer chains. However, these materials are thermoplastics, that is, they can be processed at moderate temperatures because the cross-links are reversible.^{7,8}

An interesting common feature in both single-ion conductors and thermoplastic ionomers is the presence of ion clusters. The standard methodology for detecting their presence is small-angle X-ray scattering (SAXS) and small angle neutron scattering (SANS). The typical value of the average distance between clusters, d_{cluster} is 5 nm. In Table 1 we show literature data for a wide variety of charged polymers: polymers with both strong and weak acidic groups (e.g., sulfonic vs carboxylic acid groups), polymers neutralized with metallic counterions such as

sodium and zinc, dry and hydrated polymers, crystalline and amorphous polymers, random copolymers and block copolymers.^{9–21} Also included in Table 1 is recent work on the synthesis and characterization of precise ionomers wherein the ionic groups are located periodically along the backbone.^{9,10,18,22} It is remarkable that the values of d_{cluster} obtained from all of the systems listed in Table 1 lie between 1.8 and 6.0 nm.

The purpose of this paper is to explore the effect of clustering on proton transport in PEMs. We propose that proton transport is hindered by the presence of clusters and present an approach for achieving cluster-free PEMs.

The types of polymer chains of interest are shown in Figure 1a. The simplest example is sulfonated polystyrene (PSS) with randomly functionalized styrene units along an amorphous polystyrene backbone. Also shown in Figure 1a is Nafion, a random copolymer of hydrophilic perfluoroether side chains with terminal sulfonic acid moieties, and hydrophobic tetrafluoroethylene monomers that crystallize. The last example in Figure 1a is a block copolymer comprising a PSS block and an uncharged block, polymethylbutylene (PMB). In this case, the charged monomers are confined to a portion of the chain, the PSS block.

Figure 1b and c each show a schematic of self-assembled structures formed by the random and block copolymers discussed above. Figure 1b shows clusters formed in Nafion and PSS that are present throughout the sample. Figure 1c shows clusters formed in microphase-separated PSS-PMB copolymers wherein clustering is restricted to one of the microphases. Figure 1b,c also contains an illustration of the

Received: July 30, 2012

Accepted: September 7, 2012

Published: September 14, 2012

Table 1. Ionomers from Select References, Of Varying Composition, Are Presented with a Representative Value of d_{cluster} . All of Which lie between 1.8 and 6.0 nm

monomer chemistry	abbreviation	ionomer type ^a	acid group	counterion	hydration ^b	crystallinity ^c	d_{cluster} ^d (nm)
ethylene/methacrylic acid, ethylene/acrylic acid ¹⁴	EMAA, EAA	R	CO ₂ ⁻	Li ⁺ , Na ⁺ , Cs ⁺	D	C	2.9 ± 0.6
styrene/sulfonated styrene ²⁰	PSS	R	SO ₃ ⁻	H ⁺ , Na ⁺ , K ⁺ , Zn ²⁺	D	A	3.3 ± 0.8
tetrafluoroethylene/perfluoroether sulfonic acid ¹¹	Nafion	R	SO ₃ ⁻	H ⁺	D	C	5.0 ± 0.6
ethylene oxide/sulfonated polyester ⁹	PEO/PES	P	SO ₃ ⁻	Li ⁺	D	C	2.3 ± 0
ethylene/acrylic acid ^{10,18}	EpAA	P	CO ₂ ⁻	H ⁺ , Zn ²⁺	D	C	1.8 ± 0.7
ethylene/geminal phosphonic acid ²²	EpgPA	P	PO ₃ ²⁻	H ⁺	D	C	2.4 ± 0
sulfonated styrene/ethylene/butylene ¹⁵	S-SEBS	B	SO ₃ ⁻	H ⁺ , Na ⁺ , Zn ²⁺	D	A	6.0 ± 0.3
ethylene/methacrylic acid ¹⁹	EMAA	R	CO ₂ ⁻	Na ⁺	H	C	2.1 ± 0.3
styrene/sulfonated styrene ²¹	PSS	R	SO ₃ ⁻	Zn ²⁺	H	A	4.7 ± 1.6
tetrafluoroethylene/perfluoroether sulfonic acid ¹³	Nafion	R	SO ₃ ⁻	H ⁺	H	C	4.5 ± 1.0
sulfonated α -methylstyrene/fluorinated arylene ether ¹⁶	PMSS-PAE	C	SO ₃ ⁻	H ⁺	H	A	3.0 ± 0.4
sulfonated styrene/vinylidene difluoride/hexafluoropropylene ¹⁷	PSS-PVDFcoHFP	B	SO ₃ ⁻	H ⁺ , TMA ⁺	H	A	3.7 ± 1.5
sulfonated styrene/methylbutylene ¹²	PSS-PMB	B	SO ₃ ⁻	H ⁺	H	A	3.8 ± 0.8

^aIonomer types: R, random copolymer; P, precise copolymer; B, block copolymer; C, comb copolymer. ^bHydration: D, dry ionomer; H, hydrated ionomer. ^cCrystallinity: A, amorphous; C, semicrystalline. ^dFor references that contained multiple samples, the presented value represents the middle of the range of d_{cluster} values and is followed by the difference between the extremes of that range and the middle value listed.

ionic clusters. The spherical morphology of the ionic clusters was first proposed for PSS by Yaruso and Cooper²⁰ and for Nafion by Hsu and Gierke.¹¹

To achieve adequate proton conductivity in fuel cells, PEMs are operated in the hydrated state. At low water concentrations, the ionic clusters are swollen with water. At sufficiently high water concentration one expects connections between the clusters, as shown schematically in Figure 1d. A percolated network of hydrated channels is essential for proton transport through the membrane, and the model we have adopted in Figure 1d was originally proposed by Hsu and Gierke.¹¹ In principal, the percolated channel could be devoid of clusters. However, SAXS and SANS data in the hydrated state usually contain a scattering peak that is very similar to that seen in the dry state (see Table 1). This indicates the presence of clusters in both dry and hydrated states. As indicated in Figure 1d, the consequence of the presence of clusters with an average spacing of d_{cluster} is the creation of an ion-free region of length $d_{\text{ion-free}}$; both d_{cluster} and $d_{\text{ion-free}}$ are shown in Figure 1d. An additional length scale that is important is the average distance between fixed anions that are covalently bonded to the polymer backbone, $d_{\text{fixed-ion}}$, which depends on the nature of clustering, extent of hydration, and the average number of ionic groups per chain. It is obvious that $d_{\text{fixed-ion}}$ is reduced by clustering, relative to the hypothetical case, wherein clustering is absent.

Hsu and Gierke recognized that clustering impedes ion motion.¹¹ One expects the average distance between pairs of dissociated negative and positive ions in hydrated PEMs to be about 0.7 nm, the Bjerrum length of water.²³ The passage of current requires protons to hop from one cluster to the next across regions that are devoid of ions, which is represented in Figure 1d by $d_{\text{ion-free}}$. Geometric arguments indicate that $d_{\text{ion-free}} = d_{\text{cluster}} - 2r$, where r is the radius of the clusters. Because r has not been measured in most PEMs, it is difficult to quantify $d_{\text{ion-free}}$. For PEMs with $d_{\text{cluster}} = 5$ nm (the most common value), $d_{\text{ion-free}}$ is estimated to be ~ 3 nm, assuming $r \sim 1$ nm. Support for the proposed value of r will be presented shortly. It is clear that the hopping distance ($d_{\text{ion-free}}$) is expected to be significantly greater than the Bjerrum length. In such cases, one

expects a large activation barrier for intercluster hopping. This activation barrier will not exist if clustering were avoided.

The three approaches for studying clusters are rheology, electron microscopy, and scattering. The rheological properties of ionomers are similar to those of chemically cross-linked polymers, indicating the presence of physical cross-links or ionic aggregates.^{7,24} More direct evidence for the presence of clusters should, in principle, come from electron microscopy, but this is not the case. Reasons for this include the small size of the clusters, lack of contrast between the clusters and the hydrophobic matrix, and the limited stability of polymers in an electron beam. To our knowledge, the only clear micrograph of acidic clusters in a PEM is contained in the work of Yakovlev et al.²⁵ Tomographic reconstruction of high angle annular dark field (HAADF) electron micrographs from thin films of PSS-PMB block copolymers revealed that the distribution of cluster sizes in the sample is Gaussian with an average cluster diameter of 1.4 nm. Figure 2 shows the HAADF image and the cluster distribution results from ref 25. To date there are no clear images of clusters in hydrated systems.

There have been numerous attempts to determine the morphology of clusters in hydrated random copolymers, particularly Nafion, using SAXS and SANS. There is still significant disagreement over interpretation of the scattering data because the profiles obtained in the hydrated state also contain a single broad peak. Disparate morphologies such as connected spheres,¹¹ core-shell structures,²⁶ hard spheres,²⁰ bundles of rods,²⁷ parallel cylindrical channels,²⁸ and lamellar channels²⁹ are all consistent with the observed scattering profiles. A notable exception to this is the work on precise ionomers where higher order scattering peaks, indicating the presence of long-range order, are seen.^{10,18,22} Even in this case, the structure of individual clusters (cluster form factor) was inferred from the absence of an expected scattering peak.

Studies of the morphology of ion-containing block copolymers in the hydrated state by SAXS and SANS suggest a morphology shown schematically in Figure 3a. There are two levels of microphase separation in these systems. At the higher level one obtains hydrated PSS-rich and dry PMB-rich microdomains with a characteristic length scale, d_{block} . Within

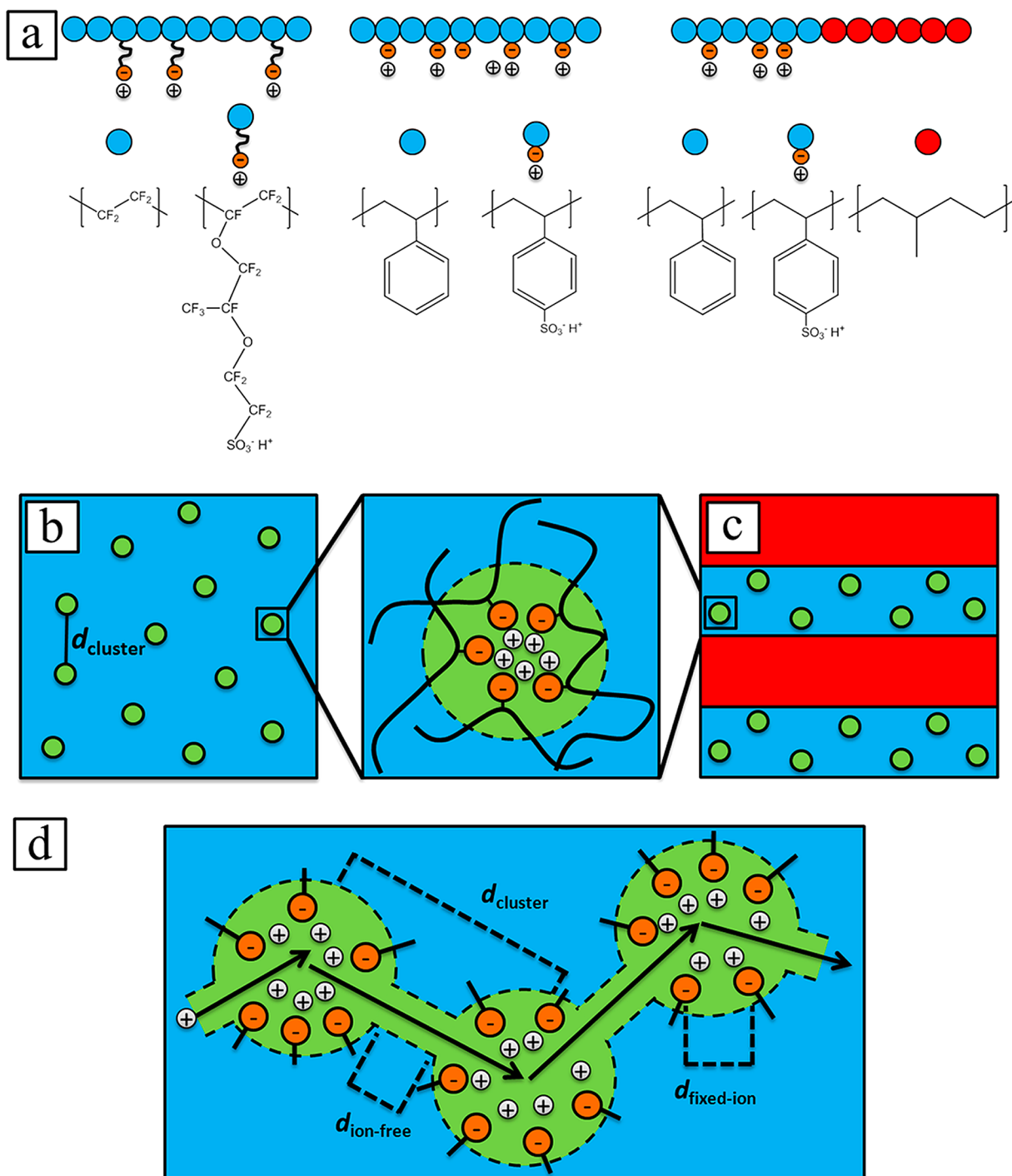


Figure 1. (a) Examples of molecular structures for different types of ionomers, from left to right: a random copolymer Nafion, a random copolymer sulfonated polystyrene (PSS), and a block copolymer sulfonated polystyrene-*block*-polymethylbutylene (PSS-PMB). Schematics of ion clusters in (b) random ionomers such as PSS and Nafion and (c) a block copolymer. The green spheres represent the ionic clusters that are a distance, d_{cluster} , apart. (d) Proton transport through a membrane containing hydrated ionic clusters a distance d_{cluster} apart, with a region free of ions between the clusters a distance $d_{\text{ion-free}}$ long, with fixed charges inside the clusters being on average a distance $d_{\text{fixed-ion}}$ apart.

the PSS-rich phase one obtains a percolated network of ion clusters and hydrated channels as proposed by Hsu and Gierke.¹¹ The morphology of ion containing block copolymers is thus governed by three length scales, d_{block} , d_{cluster} , and $d_{\text{fixed-ion}}$.

It is convenient to use SANS to study the morphology of hydrated samples due to the high contrast between D_2O and ordinary hydrogenous polymers.^{16,17} Kim et al. conducted a

systematic study of clustering in symmetric PSS-PMB copolymers. In Figure 4 we show SANS data from two hydrated samples, PSS-PMB[13–9] and PSS-PMB[5–4]. (Polymers are named according to the block molecular weights of the PSS and PMB blocks, respectively, in kg/mol.) The characteristics of these two polymer samples in the hydrated state are summarized in Table 2. The peaks marked by triangles

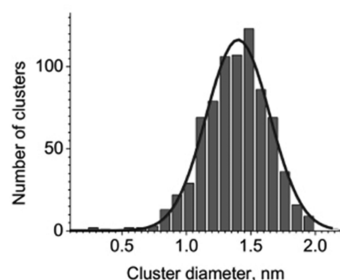
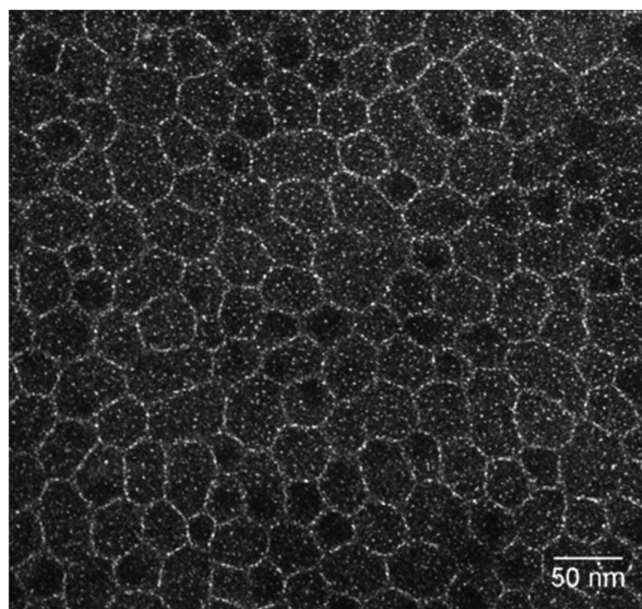


Figure 2. Electron micrograph showing acidic clusters in a dry PSS-PMB membrane and cluster size distribution determined from the micrograph. See ref 25 for details.

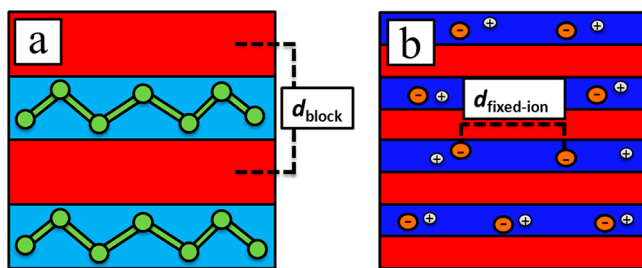


Figure 3. Schematic of the hydrated block copolymer ionomer where (a) the block copolymer domain, d_{block} , is sufficiently large that the hydrated ionic phase is equivalent to its bulk structure and (b) d_{block} is on the sample length scale as the ion cluster morphology (i.e., $d_{\text{block}}/2 \approx d_{\text{cluster}} \approx 5$ nm) resulting in a homogeneous ion phase and an increase in distance between fixed charges, $d_{\text{fixed-ion}}$.

are related to microphase separation between PSS and PMB in the presence of water. The morphology of the polymers was studied by SANS and TEM and was determined to be hexagonally packed PMB cylinders in a PSS matrix. The most important difference between the scattering curves is the presence of a cluster peak for PSS-PMB[13-9] corresponding to $d_{\text{cluster}} = 3.1$ nm (peak marked by * in Figure 4) and the absence of a cluster peak in PSS-PMB[5-4].¹² It is worth noting that the cluster peak was not seen in PSS-PMB[5-4] in both dry and hydrated states. The value of d_{block} of PSS-PMB[13-9] was 22.4 nm, while that of PSS-PMB[5-4] was

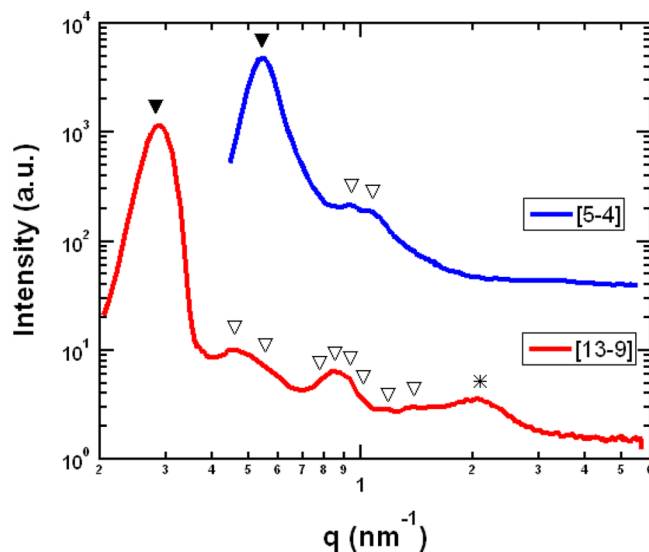


Figure 4. In situ SANS scattering intensity of hydrated PSS-PMB block copolymers plotted versus the scattering vector, q , at 60 °C and 95% relative humidity. Data for scattering profiles were obtained from ref 12 and are offset vertically for visual clarity. The position of the primary scattering peak, q_{\blacktriangledown} , is denoted by inverted filled triangles (\blacktriangledown) and is related to block copolymer domain size, d_{block} , by the relationship $d_{\text{block}} = 2\pi/q_{\blacktriangledown}$. The positions of higher order scattering peaks related to the block copolymer morphology are denoted by the inverted open triangles (\triangledown). Both samples exhibit a hexagonal morphology, while the size of d_{block} for PSS-PMB[13-9] is larger than that of PSS-PMB[5-4]. A cluster peak is observed for PSS-PMB[13-9] and is denoted by an asterisk (*), the position of this peak corresponds to a distance between clusters, d_{cluster} , of 3.1 nm. A cluster peak is absent in the scattering profile of PSS-PMB[5-4] and is due to confinement within a sufficiently small block copolymer domain.

Table 2. Summary of Morphology Properties of Polymers PSS-PMB[5-4] and PSS-PMB[13-9] Taken from Ref 12: Domain Sizes of Block Copolymer, d_{block} , in the Hydrated State, and the Distance between Ionic Clusters, d_{cluster} , in the Hydrated State^a

name	d_{block}^b (nm)	d_{cluster}^b (nm)	σ^c (S/cm) ³⁰	λ^c ³⁰
PSS-PMB[5-4]	11.6		1.6×10^{-1}	22.5
PSS-PMB[13-9]	22.4	3.1	9.1×10^{-2}	22.0

^aIon clustering is absent in PSS-PMB[5-4], and is a result of the small size of d_{block} .^bObtained at 60 °C and 95% relative humidity. ^c σ , proton conductivity and λ , the number of water per sulfonic acid group, were obtained at 60 °C and 98% relative humidity.

11.6 nm. It is evident that there is a correlation between higher level morphology and cluster formation. In particular, small values of d_{block} suppress the formation of clusters. This is shown schematically in Figure 3b where the ion-containing microphase is homogeneous. An interesting consequence of this homogenization is the increase in $d_{\text{fixed-ion}}$, as depicted in Figure 3b. The second and third columns in Table 2 summarize SANS characterization results of samples PSS-PMB[5-4] and PSS-PMB[13-9].

It is intuitively obvious that clustering will be affected by higher level self-assembly when the size of the hydrophilic domains approaches the average distance between clusters. For the case of symmetric block copolymers this occurs when $d_{\text{block}}/2 \approx d_{\text{cluster}}$. One thus expects qualitative differences in

clustering when the size of the hydrophilic phase, $d_{\text{block}}/2$ approaches 5 nm. One can qualitatively ascribe this to the well-established effect of confinement on phase separation. Liquid–liquid phase separation in the bulk is driven by free energy differences between the homogeneous state and the phase separated states. The energetic penalty associated with the formation of an interface between the phase separated states is irrelevant. However, as the size of the coexisting phases decreases the interfacial energy becomes increasingly important and when the system size decreases beyond a certain critical value, the homogeneous phase is stabilized. This was modeled by Nauman and Balsara using the Cahn–Hilliard approach, ignoring wetting interactions between the liquid and the confining medium.³¹ A more refined model that included the effect of wetting was proposed by Liu et al.³² Experiments of Lin et al. showed that confining water/lutidine mixtures within the pores of Vycor glass (pore diameter = 7 nm) resulted in homogenization.³² (Water/lutidine mixtures are phase-separated in the bulk.) Our hypothesis is that the homogenization of the ion-containing microphases in PSS-PMB[5–4] is due to the confinement of the ionic domains to 6 nm wide PSS-rich domains. We acknowledge that the phase separation of ionic clusters from nonionic chain segments is much more complicated than that of binary liquid mixtures. More work is thus necessary to confirm our hypothesis.

Incomplete dissociation of highly charged polymers in water, even at infinite dilution, is well-established.^{23,33,34} This is because the free energy of a completely dissociated, highly charged chain is larger than that of a partially dissociated chain due to the Coulombic repulsion of closely spaced negative charges that are confined to the polymer backbone. This phenomenon, often referred to as counterion condensation, occurs when the average distance between fixed charges along the polymer backbone is less than the Bjerrum length. In the case of hydrated ionomers, sulfonic acid groups are confined to the interface between the hydrophobic matrix and the hydrated channels (see Figure 1d). One expects counterion condensation on surfaces to be more significant than in linear chains due to the increased number of neighbors.^{34–36} The clustering of ions results in a small value of $d_{\text{fixed-ion}}$, which in turn increases counterion condensation.^{36,37} We thus propose that counterion condensation in PSS-PMB[5–4] is less than that in PSS-PMB[13–9] due to the larger value of $d_{\text{fixed-ion}}$.

Park et al. found that proton conductivity of hydrated PSS-PMB block copolymers was a strong function of d_{block} .³⁰ Higher conductivity was obtained when d_{block} in the dry state was lower than 12 nm. Block copolymers with such small values of d_{block} are typically difficult to achieve due to small values of Flory–Huggins interaction parameter, χ , between the two blocks. In ionic systems, however, χ is estimated to be much higher, with estimates of χ between sulfonated polystyrene and polystyrene ranging from 5.6 to 25 (typical values of χ for neutral polymer systems are much less than 0.1).^{38–40} The characterization results for PSS-PMB[5–4] and PSS-PMB[13–9] are shown in Table 2, the proton conductivity of PSS-PMB[5–4] is 1.6×10^{-1} S/cm, while that of PSS-PMB[13–9] is 9.1×10^{-2} S/cm, water uptake measurements indicate no substantial difference between the samples (the number of water molecules per sulfonic acid group, $\lambda = 22.5$ vs 22.0 for PSS-PMB[5–4] and PSS-PMB[13–9], respectively). It was noted in ref 37 that increased water retention seen in PSS-PMB block copolymers with d_{block} less than 12 nm could be attributed to capillary condensation. While this can certainly affect ion conduction,

arguments presented in this paper suggest that homogenization of ion-conducting microphases is an additional factor that affects ion transport when $d_{\text{block}} \leq 12$ nm. Homogenization increases conductivity for two reasons: (1) the absence of channels of pure water that the protons must hop across and (2) reduction of counterion condensation. We propose that eliminating clusters is one avenue for improving the conductivity of hydrated polymer electrolyte membranes. While we have focused exclusively on proton transport, similar clusters are obtained in polymeric single-ion conductors with Li^+ counterions.⁹ The relationships between clustering and ion transport that we have discussed here are also applicable to Li^+ transport.

AUTHOR INFORMATION

Corresponding Author

*E-mail: nbalsara@berkeley.edu.

Notes

The authors declare no competing financial interest.

ACKNOWLEDGMENTS

The authors thank Dr. Sergey Yakovlev and Dr. Kenneth Downing for their work imaging ion clusters in PSS-PMB block copolymers and for helpful discussions on the subject. This work was supported by the Electron Microscopy of Soft Matter Program at Lawrence Berkeley National Laboratory (LBNL) supported by the Director, Office of Science, Office of Basic Energy Sciences, Materials Sciences and Engineering Division, of the U.S. Department of Energy under Contract No. DE-AC02-05CH11231.

REFERENCES

- (1) Kreuer, K. D. *J. Membr. Sci.* **2001**, *185* (1), 29–39.
- (2) Mauritz, K. A.; Moore, R. B. *Chem. Rev.* **2004**, *104* (10), 4535–4585.
- (3) Thomas, K. E.; Sloop, S. E.; Kerr, J. B.; Newman, J. J. *Power Sources* **2000**, *89* (2), 132–138.
- (4) Nemat-Nasser, S. *J. Appl. Phys.* **2002**, *92* (5), 2899–2915.
- (5) Li, B.; Wang, L. D.; Kang, B. N.; Wang, P.; Qiu, Y. *Sol. Energy Mater. Sol. Cells* **2006**, *90* (5), 549–573.
- (6) Spurgeon, J. M.; Walter, M. G.; Zhou, J.; Kohl, P. A.; Lewis, N. S. *Energy Environ. Sci.* **2011**, *4* (5), 1772–1780.
- (7) Eisenberg, A. *Macromolecules* **1970**, *3*, 147–154.
- (8) Eisenberg, A.; King, M. *Ion Containing Polymers, Physical Properties and Structure*; Academic Press: New York, NY, 1977.
- (9) Wang, W. Q.; Liu, W. J.; Tudryn, G. J.; Colby, R. H.; Winey, K. I. *Macromolecules* **2010**, *43* (9), 4223–4229.
- (10) Baughman, T. W.; Chan, C. D.; Winey, K. I.; Wagener, K. B. *Macromolecules* **2007**, *40* (18), 6564–6571.
- (11) Hsu, W. Y.; Gierke, T. D. *J. Membr. Sci.* **1983**, *13* (3), 307–326.
- (12) Kim, S. Y.; Park, M. J.; Balsara, N. P.; Jackson, A. *Macromolecules* **2010**, *43* (19), 8128–8135.
- (13) Kusoglu, A.; Modestino, M. A.; Hexemer, A.; Segalman, R. A.; Weber, A. Z. *ACS Macro Lett.* **2012**, *1* (1), 33–36.
- (14) Macknight, W. J.; Taggart, W. P.; Stein, R. S. *J. Polym. Sci., Part C: Polym. Symp.* **1974**, *45*, 113–128.
- (15) Mani, S.; Weiss, R. A.; Williams, C. E.; Hahn, S. F. *Macromolecules* **1999**, *32* (11), 3663–3670.
- (16) Nieh, M.-P.; Guiver, M. D.; Kim, D. S.; Ding, J.; Norsten, T. *Macromolecules* **2008**, *41* (16), 6176–6182.
- (17) Rubatat, L.; Shi, Z. Q.; Diat, O.; Holdcroft, S.; Frisken, B. J. *Macromolecules* **2006**, *39* (2), 720–730.
- (18) Seitz, M. E.; Chan, C. D.; Opper, K. L.; Baughman, T. W.; Wagener, K. B.; Winey, K. I. *J. Am. Chem. Soc.* **2010**, *132* (23), 8165–8174.

- (19) Tsujita, Y.; Yasuda, M.; Kinoshita, T.; Takizawa, A.; Yoshimizu, H.; Davies, G. R. *J. Polym. Sci., Part B: Polym. Phys.* **2002**, *40* (9), 831–839.
- (20) Yarusso, D. J.; Cooper, S. L. *Macromolecules* **1983**, *16* (12), 1871–1880.
- (21) Yarusso, D. J.; Cooper, S. L. *Polymer* **1985**, *26* (3), 371–378.
- (22) Buitrago, C. F.; Opper, K. L.; Wagener, K. B.; Winey, K. I. *ACS Macro Lett.* **2012**, *1* (1), 71–74.
- (23) Manning, G. S. *J. Chem. Phys.* **1969**, *51* (3), 924–&.
- (24) Eisenberg, A.; Hird, B.; Moore, R. B. *Macromolecules* **1990**, *23* (18), 4098–4107.
- (25) Yakovlev, S.; Wang, X.; Ercius, P.; Balsara, N. P.; Downing, K. H. *J. Am. Chem. Soc.* **2011**, *133* (51), 20700–20703.
- (26) Fujimura, M.; Hashimoto, T.; Kawai, H. *Macromolecules* **1982**, *15* (1), 136–144.
- (27) Loppinet, B.; Gebel, G. *Langmuir* **1998**, *14* (8), 1977–1983.
- (28) Schmidt-Rohr, K.; Chen, Q. *Nat. Mater.* **2008**, *7* (1), 75–83.
- (29) Litt, M. H. *Polym. Prepr. (Am. Chem. Soc., Div. Polym. Chem.)* **1997**, *38* (1), 80–81.
- (30) Park, M. J.; Downing, K. H.; Jackson, A.; Gomez, E. D.; Minor, A. M.; Cookson, D.; Weber, A. Z.; Balsara, N. P. *Nano Lett.* **2007**, *7* (11), 3547–3552.
- (31) Nauman, E. B.; Balsara, N. P. *Fluid Phase Equilib.* **1989**, *45* (2–3), 229–250.
- (32) Liu, A. J.; Durianmgt, D. J.; Herbolzheimer, E.; Safran, S. A. *Phys. Rev. Lett.* **1990**, *65* (15), 1897–1900.
- (33) Dobrynin, A. V.; Rubinstein, M. *Prog. Polym. Sci.* **2005**, *30*, 1049–1118.
- (34) Toomey, R.; Tirrell, M. *Annu. Rev. Phys. Chem.* **2008**, *59*, 493–517.
- (35) Balastre, M.; Li, F.; Schorr, P.; Yang, J. C.; Mays, J. W.; Tirrell, M. V. *Macromolecules* **2002**, *35* (25), 9480–9486.
- (36) Beers, K. M.; Hallinan, D. T., Jr.; Wang, X.; Pople, J. A.; Balsara, N. P. *Macromolecules* **2011**, *44* (22), 8866–8870.
- (37) Rollet, A. L.; Diat, O.; Gebel, G. *J. Phys. Chem. B* **2002**, *106* (12), 3033–3036.
- (38) Park, M. J.; Balsara, N. P. *Macromolecules* **2008**, *41* (10), 3678–3687.
- (39) Tan, N. C. B.; Liu, X.; Briber, R. M.; Peiffer, D. G. *Polymer* **1995**, *36* (10), 1969–1973.
- (40) Zhou, N. C.; Xu, C.; Burghardt, W. R.; Composto, R. J.; Winey, K. I. *Macromolecules* **2006**, *39* (6), 2373–2379.